

Induction plasma spheroidization of tungsten and molybdenum powders

JIANG Xian-Liang (蒋显亮)¹, M. BOULOS²

1. Institute of Surface and Coatings Technology, School of Materials Science and Engineering, Central South University, Changsha 410083, China;
2. Plasma Technology Research Center, University of Sherbrooke, Sherbrooke J1K 2R1, Canada

Received 20 April 2005; accepted 27 September 2005

Abstract: The melting, evaporation and oxidation behaviors as well as the solidification phenomena of tungsten and molybdenum in induction plasma were studied. Scanning electron microscopy was used to examine the morphology and the cross section of plasma-processed powders. X-ray diffraction was used to analyze the oxides formed on the particle surface of these two metals. The influence of spray chamber pressure on the spheroidization and oxidation phenomena was discussed. The results show that fewer Mo particles than W particles are spheroidized at the same powder feed rate under the same plasma spray condition although molybdenum has a lower melting point. A small fraction of tungsten is evaporized and condensed either on the surface of tungsten particles nearby or on the wall of spray chamber. Tungsten oxides were found in tungsten powder processed under soft vacuum condition. Extremely large grains form inside some spheroidized particles of tungsten powder.

Key words: tungsten; molybdenum; induction plasma; melting; spheroidization; evaporation; oxidation

1 Introduction

The refractory metal of tungsten has the highest melting point (3 410 °C) among all metals, high specific mass (19.3 g/cm³), good erosion resistance, and low release of gases. It is a candidate material for many defense and high temperature structural applications. Also, it can be used as protective coatings for nuclear fusion reactors[1 – 6]. The refractory metal of molybdenum has a high melting point (2 620 °C), moderate specific mass (10.2 g/cm³), good toughness, and excellent scuff-wear resistance. It can be fabricated into gas turbine blades. Also, it can be sprayed into environment-protection coatings[7, 8].

The properties of tungsten and molybdenum coatings deposited by thermal spray are related to their microstructures and oxidation behaviors. Coating microstructures and oxidation behaviors are determined by spray conditions including spray distance, substrate temperature, chamber pressure, etc. Spray distance influences coating porosity and thus wear resistance[9]. Molybdenum oxides formed in the

coating is generally attributed to the oxidation of molybdenum during both flight and deposition. For a high temperature substrate, the oxidation on the surface of Mo splats/laminae during deposition has a comparable contribution to the oxide content in the coating, but for deposition on a low temperature substrate most of oxides in the coating come from the oxidation of in-flight particles[10, 11]. Low pressure plasma spray(LPPS) under argon atmosphere has been used to deposit molybdenum and tungsten coatings on different substrates[6, 12, 13]. The porosity of tungsten coating produced by low pressure plasma spray process is affected by the melting, flattening and stacking behaviors of tungsten particles. To increase coating density, the particles of fed-in powder should be complete melting, sufficient flattening, and regular overlapping on substrate.

Plasma spheroidization of powders is a good way to study the melting behavior of the refractory metals of tungsten and molybdenum. Induction plasma spray has been used in the processing of alumina, tungsten, and molybdenum[14–16]. Emphasis of this study is to compare the melting, evaporation and oxidation behaviors of tungsten and molybdenum, as well as the

solidification phenomena of these two powders during processing by induction plasma.

2 Experimental

A schematic diagram of the induction plasma spray system used for the spheroidization of tungsten and molybdenum powders is shown in Fig.1. The plasma generator is TEKNA PL50 torch composed of a ceramic plasma confinement tube and a water-cooled copper coil with four turns. The plasma was operated at the oscillating frequency of 3 MHz. Central plasma gas is argon and the flow rate is 40 L/min. Sheath plasma gas is the mixture of argon and hydrogen and the flow rate is 90 L/min Ar + 9 L/min H₂. Plasma spheroidization conditions for tungsten and molybdenum powders are shown in Table 1. The powders were axially injected into the plasma, using a high-pressure water-cooled stainless steel injector with inner diameter of 2.5 mm and outer diameter of 6.25 mm. The powder injector was located at the first turn of the induction coil.

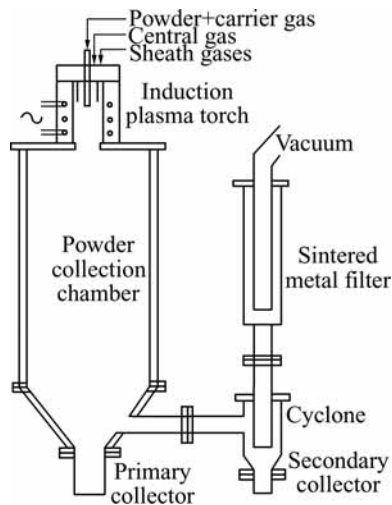


Fig.1 Schematic diagram of experimental set-up used for powder spheroidization

Table 1 Induction plasma spray condition for powder spheroidization

Powder	Plasma power/ kW	Chamber pressure/ kPa	Powder feed rate/ (g · min ⁻¹)
Tungsten	30–40	46–86	20–80
Molybdenum	30–40	46–66	25–80

The plasma spheroidization set-up consists of a powder collection chamber, a primary collector, a secondary collector, and a sintered metal filter, spheroidization set-up is connected to a plasma torch and a vacuum system. The powders were melted

inside the plasma and solidified after exiting the plasma. Molten particles of the powders would be spheroidized due to surface tension. A large fraction of the powders was collected at the bottom of the spray chamber. A small fraction of the powders was collected from the secondary collector and the chamber wall.

3 Results and discussion

3.1 Particle melting and spheroidization

Starting tungsten powder was purchased from OSRAM Sylvania Inc, USA. Starting molybdenum powder was purchased from Sulzer Metco Inc, USA. These powders consist of fused and crushed particles, as shown in Fig.2.

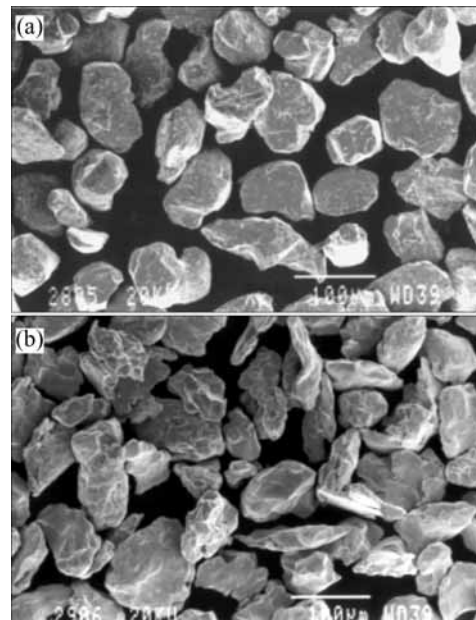


Fig.2 SEM images of starting tungsten powder (a) and molybdenum powder (b)

The heat required for complete melting of a particle can be calculated by the following equation.

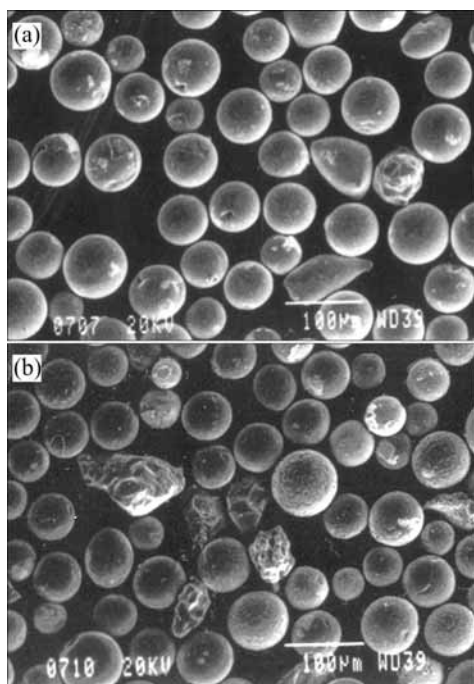
$$Q = 1/6\pi d^3 \rho [c_p (T_m - T_0) + H_m]$$

where d is particle diameter, ρ is theoretical density, c_p is specific heat, T_m is melting point, T_0 is room temperature, and H_m is latent heat of fusion. The relevant physical properties of tungsten and molybdenum are summarized in Table 2. For example, a tungsten particle with a diameter of 60 μm needs 1.41×10^{-3} J of heat energy for melting and a molybdenum particle with the same diameter needs 1.06×10^{-3} J of heat energy for melting. In other words, a single tungsten particle requires more fusion energy than a single molybdenum particle requires. However, for a given powder feed rate of 80 g/min,

Table 2 Physical properties of tungsten and molybdenum powder

Powder	Theoretical density/ ($\text{g} \cdot \text{cm}^{-3}$)	Thermal conductivity/ ($\text{W} \cdot \text{m}^{-1} \cdot \text{K}^{-1}$)	Specific heat/ ($\text{J} \cdot \text{g}^{-1} \cdot \text{K}^{-1}$)	Melting point/ $^{\circ}\text{C}$	Latent heat/ ($\text{J} \cdot \text{g}^{-1}$)
Tungsten	19.3	180	0.134	3 410	192
Molybdenum	10.2	138	0.251	2 620	288

the corresponding heat energy required for completely melting all tungsten particles is 51.6 kJ and the heat energy for completely melting all molybdenum particles is 73.7 kJ, indicating that for a given powder feed rate molybdenum powder needs more heat energy to be melted than tungsten powder needs. These energy requirements were confirmed by the experimental results that more molybdenum particles are not melted than tungsten under the same plasma processing conditions, as shown in Fig.3. It is found that some molybdenum particles have wrinkle on particle surface, indicating the temperature of the molten particles around 2 620 $^{\circ}\text{C}$ or the melting point of molybdenum.

**Fig.3** SEM images of plasma-processed tungsten powder (a) and molybdenum powder (b)

Mass fraction distributions of the powders collected from the primary collector, the secondary collector and the chamber wall are given in Table 3. The plasma processing conditions for both tungsten and molybdenum are identical, i.e., power level of 40 kW, chamber pressure of 66 kPa, and powder feed rate of 80 g/min. It can be seen from Table 3 that the mass fraction percentages of W powder collected from the primary collector and the secondary collector are

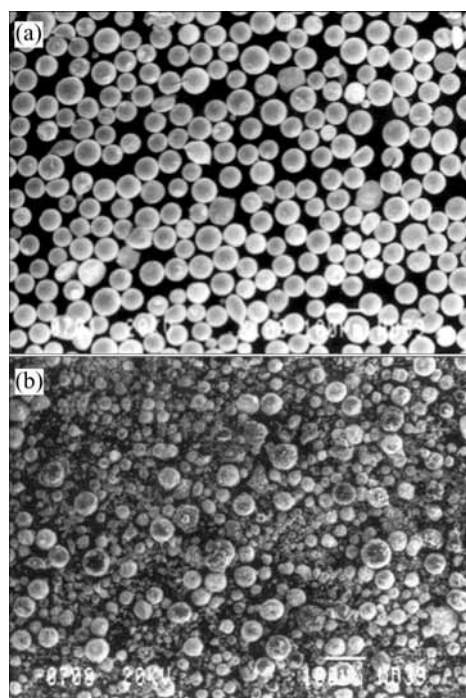
higher than those for Mo powders, respectively. However, the mass fraction of the Mo powder collected from the chamber wall is 8.9%, approximately 13 times as much as 0.7% Mo powder. The main reason is that molten Mo particles have lower viscosity and lower density and are easier sticking on the chamber wall.

Table 3 Mass fraction of W and Mo collected from different places (%)

Powder	Primary collector	Secondary collector	Chamber wall
Tungsten	92.4	6.8	0.7
Molybdenum	78.2	3.7	8.9

3.2 Evaporation and oxidation phenomena

Fig.4 shows the tungsten powders collected from the primary collector and the chamber wall. In this case, starting tungsten powder is an agglomerated powder. It can be seen from this SEM image that the powder from the primary collector has almost the same particle size as starting powder whereas the powder from the chamber wall is fine and non-uniform. This phenomenon implies that some

**Fig.4** SEM images of plasma-processed tungsten powders collected from primary collector (a) and chamber wall (b)

small particles were evaporized and condensed on the chamber wall during the plasma processing of tungsten powder. Ultrafine powder formed on the surface of large particles. As shown in Fig.5, a higher chamber pressure results in more vapor condensation on the surface of tungsten particles nearby. Chamber pressure plays an important role in the vapor condensation phenomenon.

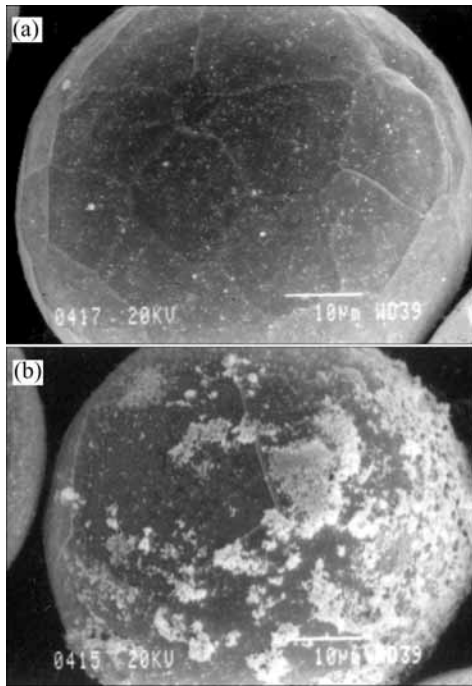


Fig.5 SEM images of tungsten particles plasma-processed at different chamber pressures: (a) 46 kPa; (b) 86 kPa

It is found that during plasma spheroidization the color of tungsten powder collected from the chamber wall is green. X-ray diffraction pattern of this powder reveals small tungsten oxide peaks, as shown in Fig.6. When the plasma spheroidization of tungsten powder is conducted under the soft vacuum condition, oxygen is believed to present in the spray chamber. Oxygen gas could come from the impurities in the plasma gases. It can also come from the leakage of plasma spray chamber. Tungsten metal is hard to be oxidized at room temperature, but is rapidly oxidized at high temperatures. High rate oxidation of tungsten particles occurs in the tail of the induction plasma where protective gas (Ar) and reduction gas (H_2) concentrations decrease and the turbulent flow of oxygen-containing gas is strong.

3.3 Solidification of molten particles

When a molten tungsten particle is at a temperature much higher than $3410\text{ }^\circ\text{C}$ or its melting point, there is sufficient time for grains to grow toward

particle center before the particle completely solidifies. As a result, some extremely large grains form. Such a behavior of grain growth is illustrated in Fig.7. Because of the orientation solidification inside the tungsten particle, pores form in the center of the tungsten particle. When the molten particle has a temperature close to the melting point of tungsten, there is no time for grains to grow during solidification. Consequently, a large number of small grains form in the tungsten particle, as shown in Fig.8.

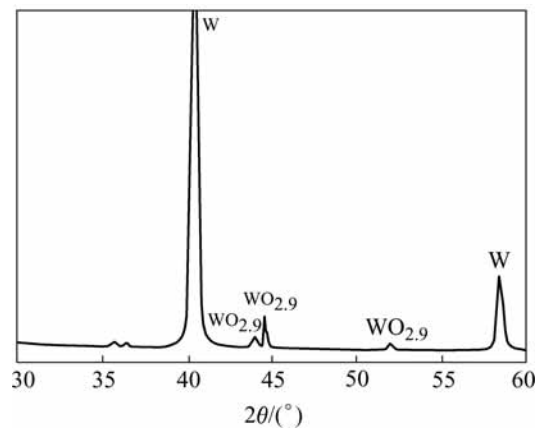


Fig.6 X-ray diffraction pattern of plasma-processed tungsten powder collected from chamber wall

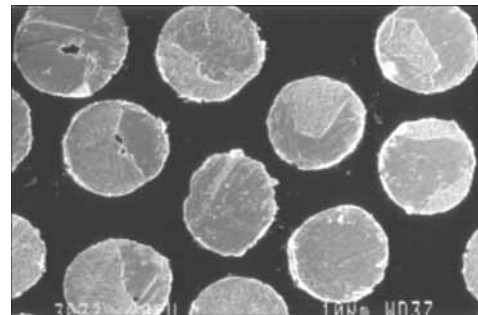


Fig.7 Cross section morphology of tungsten particles showing extremely large grains

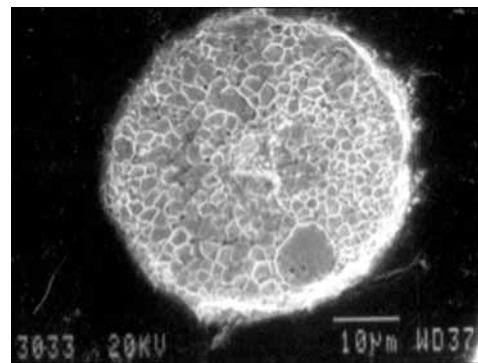


Fig.8 Cross section morphology of spheroidized tungsten particle showing large number of small grains

4 Conclusions

Induction plasma spheroidization of tungsten and molybdenum powders demonstrates that less molybdenum particles than tungsten particles are melted and spheroidized at the same powder feed rate although molybdenum has a lower melting point. When a molten tungsten particle has a temperature much higher than its melting point, some large grains form in the tungsten particle. When a molten particle has a temperature close to its melting point, a large number of small grains form in the tungsten particle. Induction plasma processing of tungsten leads to the evaporation of a limited fraction of tungsten powder. The evaporized tungsten condenses either on the wall of plasma spray chamber or on the surface of tungsten particles nearby. Oxidation of tungsten vapor occurs under soft vacuum plasma processing condition.

References

- [1] RAMAN R, THOMAS J C, HWANG D Q, et al. Design of the compact toroid fueller for center fuelling tokamak de varennes [J]. *Fusion Technology*, 1993, 24: 239–250.
- [2] JIANG X L, GITZHOFER F, BOULOS M I. Plasma spray forming of tungsten coatings on copper electrodes [J]. *Trans Nonferrous Met Soc China*, 2004, 14(5): 835–839.
- [3] BOIRE-LAVIGNE S, MOREAU C, SAINT-JACQUES R G. Taguchi analysis of the influence of plasma spray parameters on the microstructure of tungsten coatings [A]. *International Symposium on Developments and Applications of Ceramics and New Metal Alloys* [C]. Quebec City, 1993. 473–485.
- [4] MALLENER W, HOHENAUSER W, STOEVER D. Tungsten coatings for nuclear fusion devices [A]. *Proceedings of the 9th National Thermal Spray Conf* [C]. Cincinnati, 1996. 1–6.
- [5] CAVASIN A, BRZEZINSKI T, GRENIER S, et al. W and B₄C coatings for nuclear fusion reactors [A]. *International Thermal Spray Conf* [C]. France: Nice, 1998. 957–962.
- [6] KHAN A A, LABBE J C, GRIMAUD A, et al. Molybdenum and tungsten coatings for X-ray targets obtained through the low-pressure plasma spraying process [J]. *Journal of Thermal Spray Technology*, 1997, 6 (2): 228–234.
- [7] KOUTSOMICHALIS A, BADEKAS H. Corrosion behavior of molybdenum plasma spray coatings on steel [J]. *Scripta Metall Mater*, 1993, 29(8): 1125.
- [8] TJONG S C, KU T S, WU C S. Corrosion behavior of laser consolidated chromium and molybdenum plasma spray coatings on Fe-28Mn-7Al-1C alloy [J]. *Scripta Metall Mater*, 1994, 31(7): 835.
- [9] STOLARSKI T A, TOBE S. The effect of spray distance on wear resistance of Mo coatings [J]. *Wear*, 2001, 249: 1096–1102.
- [10] WAN Y P, FINCKE J R, JIANG X Y, et al. Materials processing – modeling of oxidation of molybdenum particles during plasma spray deposition [J]. *Metallurgical and Materials Transaction B*, 2001, B32: 475–482.
- [11] JIANG X, MATEJICEK J, SAMPATH S, et al. Substrate temperature effect on the splat formation, microstructure development, and properties of plasma sprayed coatings, part II: case study for molybdenum [J]. *Mater Sci Eng A*, 1999, 272: 189–198.
- [12] CAI W, LIU H, SICKINGER A, et al. Low-pressure plasma deposition of tungsten [J]. *Journal of Thermal Spray Technology*, 1994, A3(2): 135–141.
- [13] JIANG X L, BOULOS M I. Particle melting, flattening, and stacking behaviors in the induction plasma deposition of tungsten [J]. *Trans Nonferrous Met Soc China*, 2001, 11(5):811–816.
- [14] FAN X B, GITZHOFER F, BOULOS M I. Statistical design of experiments for the spheroidization of powdered alumina by induction plasma processing [J]. *Journal of Thermal Spray Technology*, 1998, 7: 247–253.
- [15] JIANG X L, TIWARI R, GITZHOFER F, et al. On the induction plasma deposition of tungsten metal [J]. *Journal of Thermal Spray Technology*, 1993, 2: 265–270.
- [16] JIANG X L, BOULOS M I. Radio frequency induction plasma spraying of molybdenum [J]. *Plasma Science & Technology*, 2003, 5: 1895–1900.

(Edited by LONG Huai-zhong)